JOURNAL OF MATERIALS SCIENCE 20 (1985) 1310–1320

On the pressure forming of two superplastic alloys

K. S. K. CHOCKALINGAM, M. NEELAKANTAN, S. DEVARAJ, K. A. PADMANABHAN
Department of Metallurgical Engineering, Indian Institute of Technology, Madras 600036, India

Superplastic forming of the Ti–6Al–4V and Sn–Pb eutectic alloys was attempted using the pressure forming (sheet thermoforming) process. It has been demonstrated that true hemispheres could be formed out of sheets of both the alloys. The thickness strains in both the alloys were less than those predicted theoretically and this could be traced to material flow from the flange and gripped regions. This flow, however, was greater in case of the titanium alloy than the Sn–Pb alloy, on account of the greater strain-rate sensitivity of the former material. Due to the same effect, the "thinning factor" actually increased with deformation in the titanium alloy, but it decreased on increasing deformation in the Sn–Pb alloy. Within the experimental range, the hold-down pressure (titanium alloy) and initial sheet thickness (Sn–Pb alloy) had very small effects, although the deformation became slightly more uniform on decreasing the hold-down pressure or increasing the initial sheet thickness. The thickness and circumferential strains increased with deformation and in particular when the bulge height (h_0) to base diameter (D_0) ratio was greater than 0.35, non-uniformity in deformation along the bulge profile became noticeable. These strains were largest at the pole and its vicinity. On account of its lower strain-rate sensitivity, these effects were more pronounced in the Sn–Pb alloy than in the titanium alloy. Although initially the bulging rate was rapid, later the (h_0/D_0) ratio increased linearly with the forming time and at any instant the bulge profile corresponded to an arc of a circle.

1. Introduction

Structurally superplastic flow [1, 2] is characterized by enormous stretchability and a very low flow stress. It occurs in metallic materials having a stable, ultra-fine grain size undergoing deformation at temperatures approximately equal to or greater than $0.4\,T_M$, where T_M is the absolute melting or phase transformation point.

The number of commercial superplastic alloys is on the increase and the unique properties obtainable during superplastic flow have been exploited in forming [2–6]. The resemblance to the behaviour of thermoplastics above their glass transition temperatures has, on the other hand, enabled the use of techniques common in polymer processing, e.g. pressure forming [2].

The early study of Backofen *et al.* [7], which reported for the first time the bulging of a superplastic alloy using a small air pressure, drew pointed attention to the strain-rate sensitive nature of flow.

Analyses for the bulging of circular diaphragms of a strain-hardening material are due to Hill [8], Swift [9] and Mellor [10]. Bramley and Mellor [11] extended the scope to cover anisotropic materials. Both theory and experiments indicate that when the clamping ring has an adequate corner radius, instability first occurs at the pole.

Bulging of the superplastic alloy sheets, which do not work harden significantly, is analysed using a constitutive equation of flow:

$$\sigma = K\dot{\epsilon}^m \quad (1)$$

0022–2461/85 $03.00 + .12

where σ is the applied stress, $\dot{\epsilon}$ is the strain rate, m is the strain-rate sensitivity index and K is a material constant. Both m and K are critically dependent on the experimental variables like strain rate, grain size and temperature. The analyses predict the bulge profiles, thickness distributions and forming and rupture times as functions of pressure, geometry and the material parameters m and K [3, 5, 6, 12, 13].

The geometry of the bulge profile is a major concern. Tang and Robbins [5] and Holt [12] have assumed the profile to be circular, while Johnson *et al.* [14] have experimentally demonstrated by forming bubbles of different heights that the free surfaces have an essentially spherical shape.

Following both theoretical and experimental investigations, Clemas *et al.* [15] have, on the other hand, concluded that the centre line profile forms an arc of a circle whose mean radius, $\bar{r}$, can be calculated from the relation

$$\bar{r} = \frac{a^2 + h^2}{2h} \tag{2}$$

where a is the base radius and h is the bulge height.

Control of non-uniformity in the thickness of the formed component is of primary importance. Cocks *et al.* [16] have examined the effect of pressure and temperature on the bulge forming of (superplastic) copper alloys, while Mamalis *et al.* [17] have studied the forming behaviour when a re-entrant die was used. Johnson *et al.* [14] recommend the use of multistage forming for most efficient control of thickness.

Contrary to experimental results, Jovane [3] has assumed that the thickness remains uniform, which invalidates a major part of his analysis. In contrast, Cornfield and Johnson [13] have used a simple parameter, the "thinning factor", to characterize the departure from uniform thinning at any given point. The thinning factor is defined as equal to $S/\bar{S}$, where S is the actual thickness and $\bar{S}$ is the (average) thickness to which the material right above the die cavity would thin down, if it were to deform uniformly at constant volume.

The present investigation is concerned with the pressure forming (sheet thermoforming) of the commercially important Ti–6Al–4V alloy and the Sn–Pb eutectic alloy, which is a model material that is superplastic at room temperature. The effects of the forming variables on the thickness strain, thinning factor, bulge profile, circumferential strain and bulge height have been studied.

2. Experimental procedure

The titanium alloy (IMI 318) had a composition (wt %) of 6.35 aluminium, 4.43 vanadium, 0.22 iron, 0.02 carbon and balance titanium. The sheet thickness was 1.64 mm and the average two-dimensional grain size was $7.9 \pm 0.2\,\mu$m. These sheets were formed in the as-received condition at 950° C.

The Sn–Pb eutectic alloy was air melted using tin and lead of commerical purity. Chill cast ingots of dimensions 140 mm x 120 mm x 15 mm were hot rolled at room temperature by different amounts to obtain sheets of thickness 1.3, 1.48 and 1.6 mm. The corresponding average two-dimensional grain sizes were 2.6 ± 0.1, 3.4 ± 0.2, $4.1 \pm 0.2\,\mu$m. Superplastic forming in this case was at room temperature.

The experimental set-up for pressure forming is shown in Fig. 1. The top chamber holds the gas (argon for the Ti–6Al–4V and air for the Sn–Pb alloys) at the desired forming pressure. The bottom die contains a cavity of the same configuration as the required component – in this case a hemisphere of 80 mm radius.

Using suitable spacers and fixtures, the top and bottom chambers were mounted coaxially onto the platens of a 35.6 tonne hydraulic press, capable of applying constant loads during the entire forming operation.

A blank of 250 mm diameter was inserted between the two chambers and an outer ring of width 15 mm was held by applying a suitable hold-down pressure. Material of 220 mm diameter was available inside for deformation into the die cavity. Some slipping of the material held between the chambers was also possible.

In the case of the titanium alloy the chambers were surrounded by a split furnace capable of reaching 1200° C. To avoid grain growth, the sheet was inserted only after the chambers had reached the forming temperature. The sheet was held at this temperature for 10 min before forming. To prevent oxidation, the bottom die cavity was evacuated and flushed with argon (through a vent hole) at least twice. In the top chamber, a gas pressure of 0.3 to 0.6 MPa (50 to 100 psi) was applied for forming. The gas escaping from the vent hole in the bottom die was led through a pipe into a water bottle. Cessation of bubble

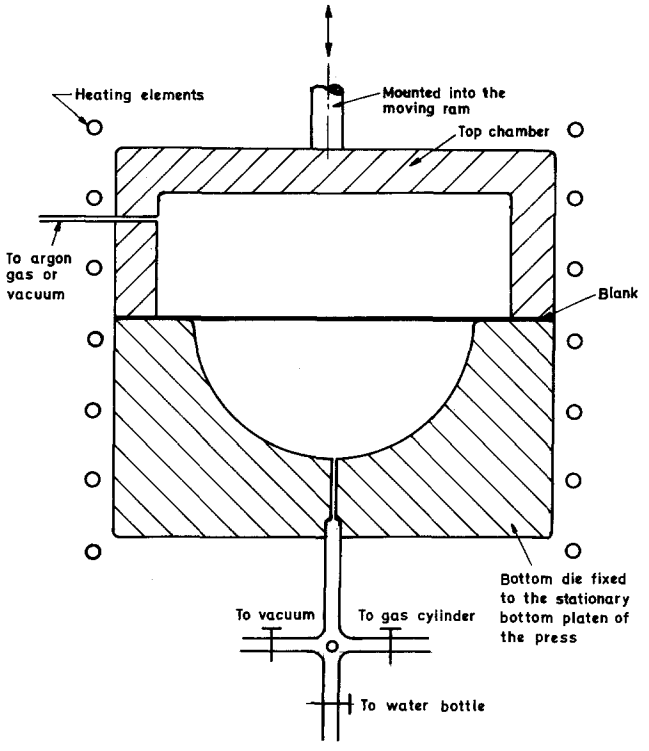

Figure 1 A schematic diagram of the experimental set-up.

formation in the water bottle indicated the completion of forming.

Sheets of the Sn–Pb alloy were screen printed to obtain grid circles and radial lines on the surface. After forming, the strain distribution was estimated by measuring the changes in the lengths of the various curves and lines. (Such a study was not possible in the case of the titanium alloy because at high temperatures the grids and lines got obliterated.)

Using a dial gauge with ball contacts, the thickness of the component formed was measured along two orthogonal diametral arcs on the bulge profile (without sectioning the domes) to an accuracy of ± 0.01 mm. Thus for a given vertical distance from the base line, four points could be located (two on each arc). This enabled verification of the symmetrical shape of the component formed.

One dome was sectioned on a diametral plane and de-burred. The thickness on each half of the dome was then measured at predetermined positions with the help of a micrometer. It was established that the maximum error in the thickness measurements was ± 3%. Circumferential strain, on the other hand, was estimated using a pair of engineers' dividers and a steel rule to an accuracy of ± 0.1 mm.

3. Results and discussion

3.1. Component

Both the Ti–6Al–4V and Sn–Pb alloy sheets formed true hemispheres. Fig. 2 shows components made of the Ti–6Al–4V alloy in the various stages of forming a hemisphere and Fig. 3 displays a completely formed hemisphere of the Sn–Pb alloy.

3.2. Thickness strain

The thickness strain is defined as $\ln (S/S_0)$, where S is the actual thickness at a given point and S_0 is the initial thickness. The non-dimensional fractional height is h/h_0, where h_0 is the height of the pole and h is the height of the given point above the base line. In Figs. 4a and b the $\ln (S/S_0)$

Figure 2 A photograph showing the various stages of formation of the Ti–6Al–4V alloy hemisphere at 950° C. Forming pressure = 0.6 MPa.

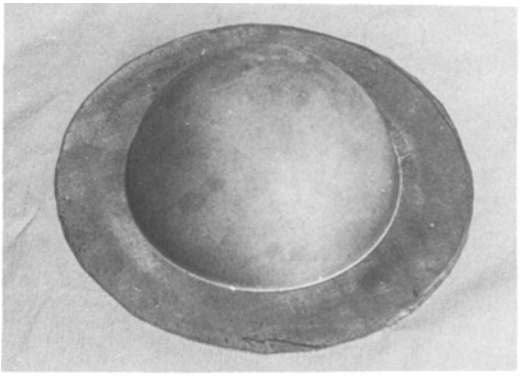

Figure 3 A photograph showing a completely formed hemisphere (at room temperature) of the Sn–Pb alloy. Initial sheet thickness 1.3 mm. Forming pressure = 0.2 MPa.

against h/h_0 relationship is presented for the titanium and Sn–Pb alloys respectively, along with theoretical variations predicted by Cornfield and Johnson [13] for $m = 0.75$ for the titanium alloy [18] and $m = 0.4$ for the Sn–Pb alloy [19].

The observed thickness strains for both the alloys were less than those predicted theoretically. Similar results have also been obtained by Cornfield and Johnson [13] and Cocks *et al.* [16].

The results could mean (1) that the value of m under conditions of bulging is different from that in tensile testing, or (2) that material from the gripped and flange portions was also flowing to take the hemispherical shape, apart from the circular disc directly above the die cavity, or (3) both. (In the analysis of Cornfield and Johnson

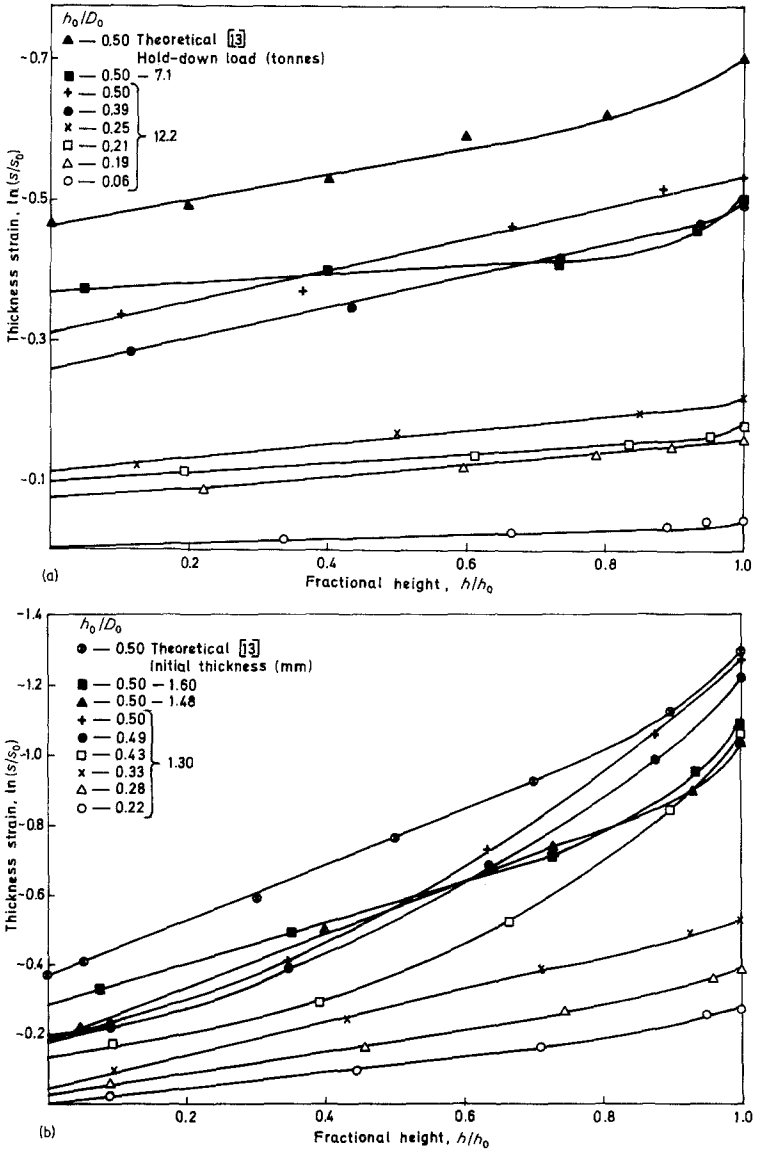

Figure 4 (a) Thickness strain as a function of fractional height for different experimental conditions. Ti–6Al–4V alloy. Forming pressure = 0.6 MPa. (b) Thickness strain as a function of fractional height for different experimental conditons. Sn–Pb alloy. Hold-down load = 7.1 tonne. Forming pressure = 0.2 MPa.

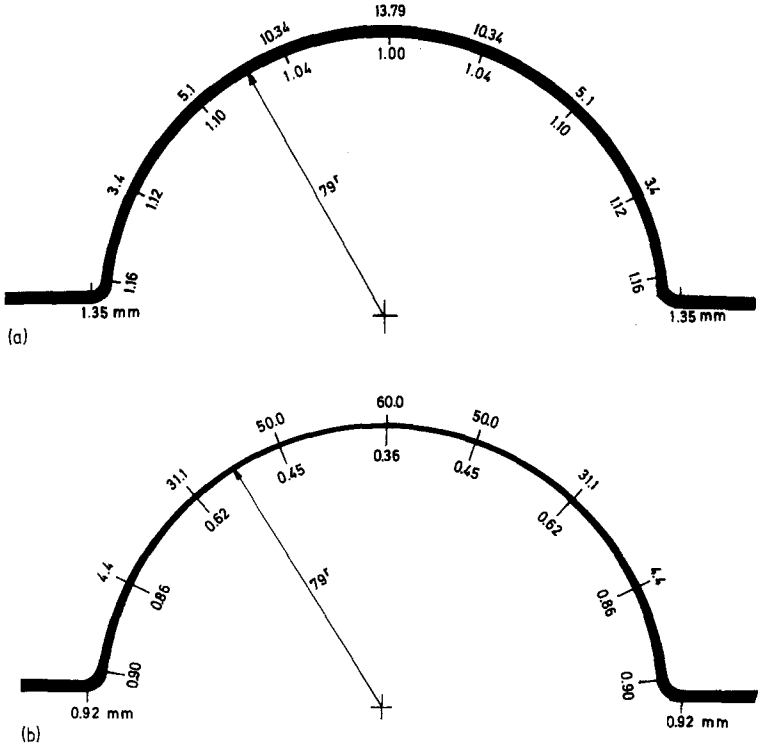

Figure 5 (a) Thickness and percentage variation of strain along a diametral section of a hemisphere of the Ti–6Al–4V alloy. Hold-down load = 7.1 tonne. Forming pressure = 0.6 MPa. (b) Thickness and percentage variation of strain along a diametral section of a hemisphere of the Sn–Pb alloy. Initial sheet thickness = 1.30 mm. Hold-down load = 7.1 tonne. Forming pressure = 0.2 MPa.

[13] only the portion directly above the die cavity is assumed to deform.)

In the present experiments, inside the gripped portion a disc of 220 mm diameter was available for flowing into the die cavity. Near the clamped edge, the thickness had reduced from 1.64 to 1.35 mm in the case of the titanium alloy, while the coresponding figures were 1.30 and 0.92 mm respectively for the Sn–Pb alloy (Figs. 5a and b). It is also clear from Fig. 4a that the thickness of the formed component becomes more uniform as the hold-down load is reduced. Thus, some drawing-in of the material gripped between the die halves was also possible, apart from the deformation of the flange portion. The complex nature of flow, however, prevented verification as to whether m also changed as the mode of testing was changed from uniaxial tension to bi-axial bulging.

The effect of initial sheet thickness is shown in Fig. 4b. The thickness strain appears to be nearly independent of the initial thickness, although for large values of the h/h_0 ratio the present results could mean that the uniformity in thickness was slightly improved on increasing the sheet thickness. It is cautioned, however, that this statement should not be held as valid beyond the present experimental range because a higher initial thickness implies a coarser grain size (due to less working) which could reduce the superplastic response.

In Fig. 4 the thickness strain is also presented as a function of the h/h_0 ratio, for different values of h_0/D_0 (D_0 = the base diameter), i.e. for different stages of forming the hemisphere. The thickness strain increased with increasing values of the h_0/D_0 ratio. When $(h_0/D_0) \gtrsim 0.35$, the increase was quite rapid, particularly near and at the pole. Finally, as the thickness strain at the pole had the highest value, its magnitude decided the acceptability or otherwise of an operation, i.e. the thickness strain at the pole is the practical forming limit parameter.

The thickness variation along a diametral section is shown in Figs. 5a and b respectively for the titanium and Sn–Pb alloys. The thickness is shown on the inside; the percentage decrease in thickness, from edge to pole, on the outside. Similar curves for a different hold-down load (titanium alloy) and sheet thickness (Sn–Pb alloy) can be derived from Figs. 4a and b respectively.

When the sheet being formed touches the die wall, the portion in contact gets supported by the normal reaction. Then, subsequent forming of the unsupported portion will involve both bulging and drawing along the (bottom) chamber wall. This

explains why the thickness decreases as one goes from the edge to pole. It is also reasonable that the thickness variation is greater for the Sn–Pb alloy ($m = 0.4$) than for the titanium alloy ($m = 0.75$), because the greater strain-rate sensitivity of the latter alloy makes it more resistant to localized thinning.

3.3. Thinning factor

The thinning factor, $(S/\bar{S})$ (Section 1), is plotted against the fractional height h/h_0 in Figs. 6a and b respectively for the titanium and Sn–Pb alloys. The thinning factor at the pole had a value of about 1.2 for the titanium alloy for both values of the hold-down load. However, for the two thicker sheets of the Sn–Pb alloy the corresponding value was about 0.7. In case of the Sn–Pb sheet of thickness 1.3 mm, the thinning factor at the pole was 0.55. The respective values for the titanium and Sn–Pb alloys, according to the theoretical calculations of Cornfield and Johnson [13], were 0.85 and 0.6.

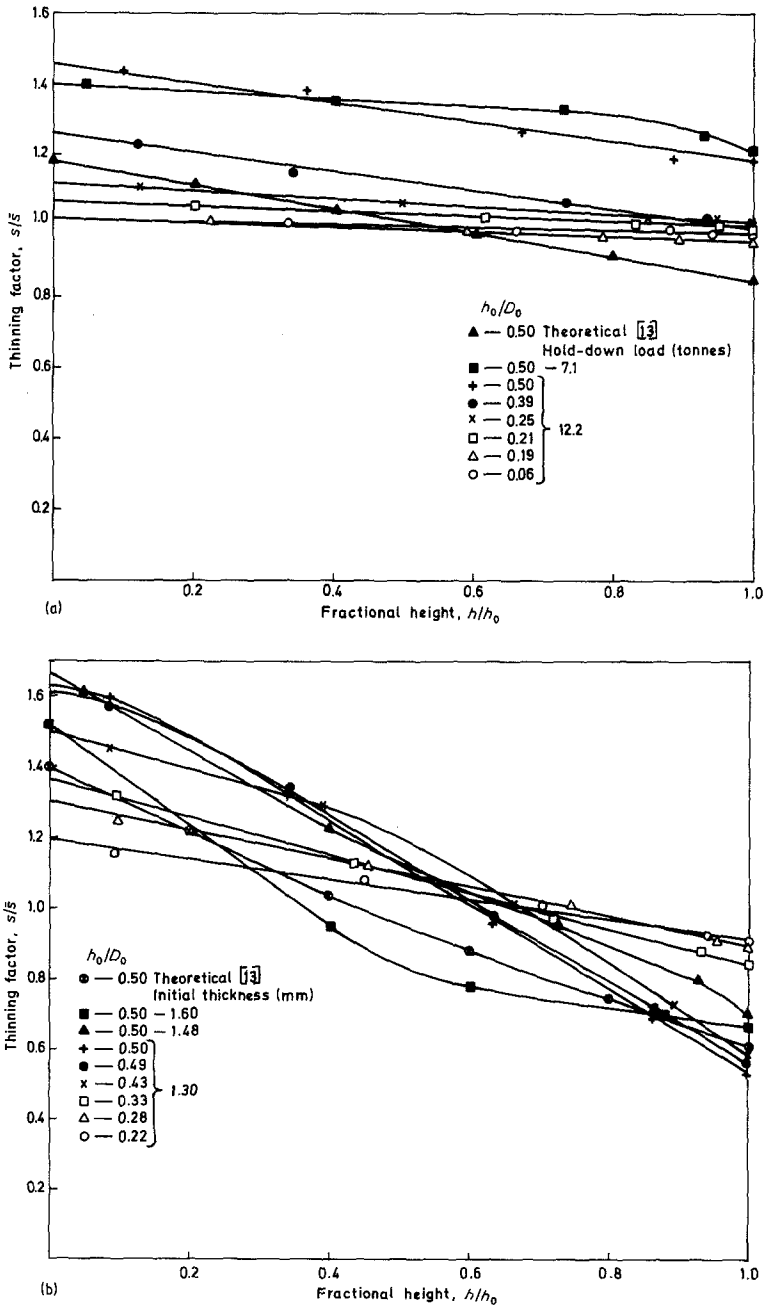

Figure 6 (a) Thinning factor as a function of fractional height for different experimental conditions. Ti–6Al–4V alloy. Forming pressure = 0.6 MPa. (b) Thinning factor as a function of fractional height for different experimental conditions. Sn–Pb alloy. Hold-down load = 7.1 tonne. Forming pressure = 0.2 MPa.

Further, in the titanium alloy the thinning factor was practically independent of the h/h_0 ratio – particularly when a smaller hold-down load was employed (Fig. 6a). Moreover, with increasing deformation (increasing h_0/D_0 values) the thinning factor actually increases, presumably due to greater flow from the flange and gripped portions on increasing the degree of deformation.

However, in the Sn–Pb alloy (Fig. 6b) the thinning factor decreases on increasing the (h_0/D_0) ratio, indicating that additional flow from the flange and gripped portions is not taking place rapidly to offset the thinning resulting from increased and localized deformation. However, the decrease in the thinning factor with increasing h_0/D_0 ratio is somewhat less for the two thicker sheets compared with the sheet of thickness 1.3 mm (possibly because of the higher m-values associated with the thicker sheets).

The difference in the behaviour of the two alloys is attributable to the difference in their m-values. In the titanium alloy the higher m-value (= 0.75) confers greater (localized) thinning resistance and nearly uniform flow in the central, flange and gripped portions results. Then the thinning factor is practically independent of the h/h_0 ratio and increases with the h_0/D_0 ratio. A similar situation has also been reported [20] during the extrusion of a superplastic alloy, wherein it has been noted that when $m \gtrsim 0.45$ the strain-rate effects were relatively unimportant. But in the Sn–Pb alloy m was only of the order of 0.4 and here the resistance to localized thinning was not high and the thinning factor decreased with increasing h/h_0 and h_0/D_0 ratios.

The theoretical relationships, based on the analysis of Cornfield and Johnson [13] – assuming $m = 0.75$ for the titanium alloy and $m = 0.4$ for the Sn–Pb alloy – are also shown in Figs. 6a and b respectively. The theoretical thinning factor is calculated assuming that only the disc of material right above the die cavity (of 160 mm diameter in this case) deforms to produce the hemispherical shape. If this disc of material were to deform uniformly, a final thickness of 0.82 mm would be predicted in the case of the hemisphere formed from the titanium alloy. The corresponding figures for the Sn–Pb alloy sheets of thickness 1.6, 1.48 and 1.3 mm would be 0.8, 0.74 and 0.65 mm respectively. However, the actual thickness at the pole (lowest value) for the titanium and Sn–Pb alloys were around 1.00 mm (hold-down load = 7 tons, i.e. 7.1 tonnes) and 0.36 mm (initial sheet thickness 1.3 mm) respectively.

It has already been stated that inside the gripped region a disc of 220 mm diameter (including flange portion) is available for deformation. If this entire region were assumed to deform uniformly, in case of the titanium alloy a final thickness of 1 mm would be predicted for the hemisphere, which was the thickness observed at the pole, when the hold-down load was 7.1 tonnes. For this case, a thinning factor of 1.2 would be predicted, which is what has been reported for both the hold-down loads. However, this approximate calculation cannot account for the observed variations in the thickness of the formed component at different points along the bulge profile.

The above calculation cannot also apply for the Sn–Pb alloy, in which the somewhat low value of m does not allow significant flow from the flange portion so much so that the thickness at the pole of the formed component is considerably less than the values predicted for all the three initial sheet thicknesses, by using the formula of Cornfield and Johnson [13].

3.4. Bulge profile

In case of both the titanium and Sn–Pb alloys, forming was stopped at different values of the h_0/D_0 ratio, i.e. at different stages in the forming of the hemisphere. For a diametral section, the dome height at regular intervals along the base diameter (where the measurement starts from one end of the diameter) was measured. The results are presented in Fig. 7a for the titanium alloy and Fig. 7b for the Sn–Pb alloy. It was also ascertained that the dome height was symmetrical about the pole.

Using geometrical construction, it was established that each curve in Figs. 7a and b formed an arc of a circle. The radius of curvature was measured. The radius of the curvature was also calculated using Equation 2. The values obtained by both the methods agreed very well (Table I). Thus the earlier supposition [5, 12, 15, 21] that the bulge profile always corresponded to an arc of a circle receives experimental support. In this connection, it must, however, be noted that when the rate sensitivity of flow is *low* bulging into a circular cavity often leads to bubbles that are conical rather than spherical [6].

3.5. Microforming

The microforming behaviour of the Sn–Pb alloy

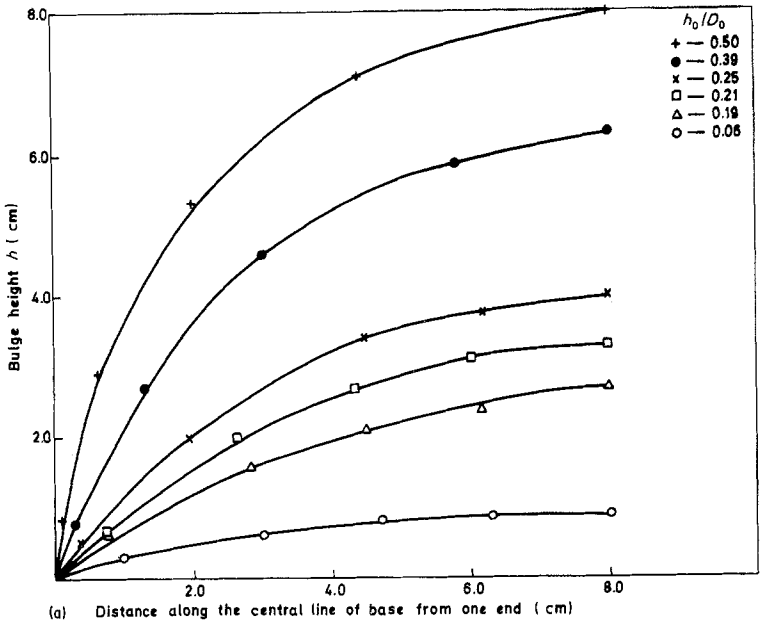

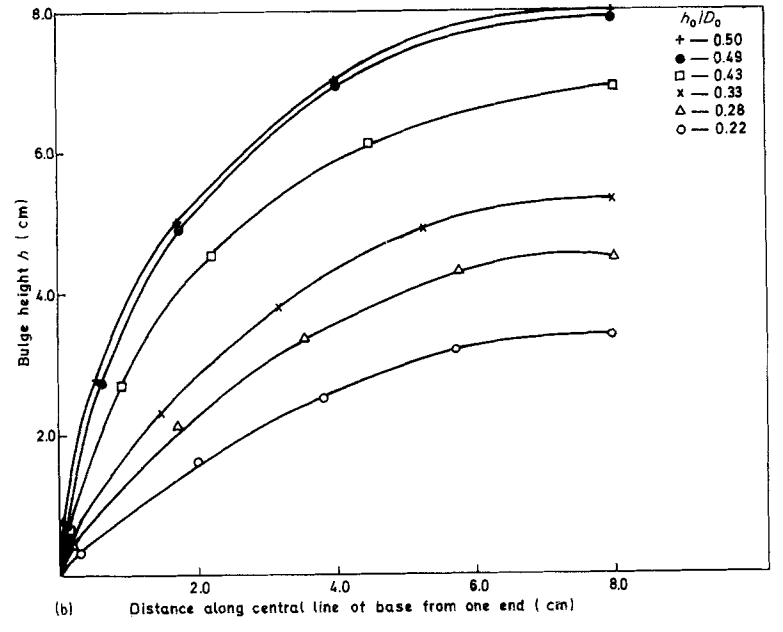

Figure 7 (a) Bulge height from the central base line of the dome at various stages of formation of the Ti–6Al–4V alloy hemisphere. Hold-down load = 12.2 tonne. Forming pressure = 0.6 MPa. (b) Bulge height from the central base line of the dome at various stages of formation of the Sn–Pb alloy hemisphere. Initial sheet thickness = 1.3 mm. Hold-down load = 7.1 tonne. Forming pressure = 0.2 MPa.

will be reported elsewhere. For the present, the ease of forming fine topographical details is demonstrated in Fig. 8, wherein the emblem of the institute of the authors is reproduced.

3.6. Circumferential strain

In case of the Sn–Pb alloy, using the grid method (Section 2) the circumferential strain was estimated as a function of the fractional height (h/h_0) – Fig. 9. It was clear that the circumferential strain near the edges was less than that near the pole and that when the bulge height to base diameter ratio exceeded 0.35, the circumferential strain near the pole became quite pronounced. This conclusion was in conformity with that reached from the other studies involving variations in the thickness strain and thinning factor (see earlier).

3.7. Bulge height

The bulge height at failure in the Sn–Pb alloy for different forming pressures at room temperature

Figure 8 A photograph showing an emblem microformed from the Sn–Pb alloy sheet. Initial thickness = 1.05 mm. Average two-dimensional grain size = 1.2 ± 0.1 μm. Forming pressure = 0.2 MPa.

TABLE I Calculated and measured values of the radius of curvature, base radius of the hemispherical dome = 80 mm

Material	Bulge height, h (mm)	Radius of curvature (mm)	
		Calculated from Equation 2 of text	Measured graphically
Ti–6Al–4V	9.0	360.1	361.0
	26.8	132.8	133.0
	32.6	114.5	115.0
	40.0	100.0	100.0
	63.0	82.3	83.0
	80.0	80.0	80.0
Sn–Pb	35.0	108.6	109.0
	45.0	93.6	94.0
	53.0	86.8	87.0
	68.0	81.1	81.5
	78.0	80.0	80.5
	80.0	80.0	80.0

is shown in Fig. 10. At a pressure of 0.2 MPa the hemispherical shape could be obtained; but at higher pressures failure occurred before this stage was reached.

At a pressure of 0.2 MPa, the bulge height to base diameter ratio (h_0/D_0) obtained as a function of the forming time is presented in Fig. 11. Initially the bulge rate was rapid, but later the h_0/D_0 ratio increased linearly with forming time. The hemispherical shape was obtained in 19 min.

4. Conclusions

Based on the present sheet thermoforming experiments on the Ti–6Al–4V and Sn–Pb eutectic alloys, the following conclusions could be drawn.

1. Using the sheet thermoforming process at the appropriate temperature and pressure, true hemispheres could be formed out of sheets of both the alloys.

2. The observed thickness strains in both the alloys were less than those predicted by an earlier analysis given by Cornfield and Johnson [13], due to material flow taking place from the flange and gripped regions (in addition to that from the central regions). This discrepancy, however, was more in the case of the titanium alloy (than the Sn–Pb alloy) because the greater strain-rate sensitivity of flow in the former alloy (m = 0.75, as against m = 0.4 for the Sn–Pb alloy) permitted more flow from the flange and gripped regions.

3. In the case of the Sn–Pb alloy, the thickness strain was nearly independent of the initial sheet

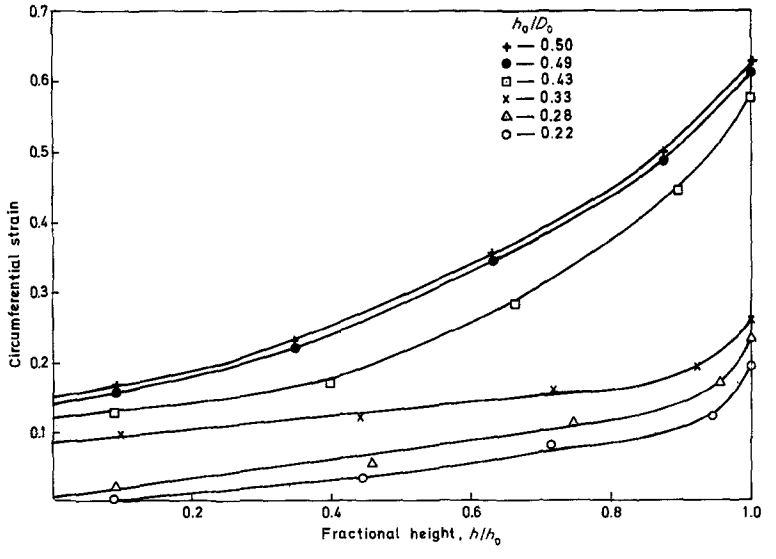

Figure 9 Circumferential strain against the fractional height, for different experimental conditions. Sn–Pb alloy. Initial sheet thickness = 1.3 mm. Hold-down load = 7.1 tonne. Forming pressure = 0.2 MPa.

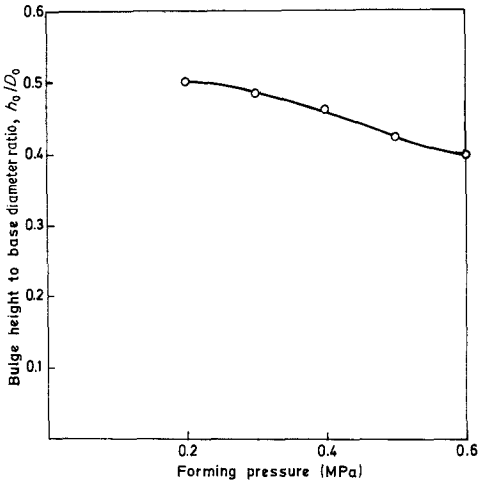

Figure 10 Bulge height at failure for different forming pressures. Sn–Pb alloy. Initial sheet thickness = 1.48 mm. Hold-down load = 7.1 tonne.

thickness. However, the deformation did appear to be slightly more uniform with two thicker sheets, perhaps due to their greater rate sensitivity of flow.

In the titanium alloy, a lower hold-down load of 7.1 tonne gave rise to slightly more uniform deformation in the hemisphere than a hold-down load of 12.2 tonne.

4. The thickness strain at fixed locations along the bulge profile increases as the bulge height (h_0) to base diameter (D_0) ratio increases, particularly beyond $h_0/D_0 > 0.35$. The thickness strain increases from the edge to the pole, where the strain reaches its maximum value. Non-uniformity in thickness along the bulge profile as well as its increase with increasing dome height is more pronounced in the Sn–Pb alloy than in the titanium alloy, again due to the lower strain-rate sensitivity of the former alloy.

5. In all cases, the observed thinning factor was more than that calculated using the approach of Cornfield and Johnson [13], due to flow also being present in the flange and gripped regions. However, flow in these regions was more in the case of the titanium alloy, which had a greater strain-rate sensitivity. Therefore, the thinning factor increased with deformation in the titanium alloy, but decreased with increasing deformation in the case of the Sn–Pb alloy.

6. In the case of both the alloys, the bulge profile at any instant corresponded to an arc of a circle, which verified an earlier assumption in this regard.

7. In the Sn–Pb alloy, circumferential strain increased with deformation and as the h_0/D_0 ratio exceeded 0.35 the increase in the circumferential strain near and at the pole was rather steep.

8. During constant pressure bulging of the Sn–Pb alloy sheet, the initial rate of bulging was rapid, but later deformation proceeded at a slower rate and the h_0/D_0 ratio increased linearly with forming time.

Acknowledgements

The authors thank the Aeronautics Research and Development Board, Ministry of Defence, Government of India, for financial support for this work. One of the authors (KSKC) thanks the Directorate of Technical Education, Tamil Nadu, for study leave under the Quality Improvement Programme of the Government of India.

References

1. J. W. EDINGTON, K. N. MELTON and C. P. CUTLER, *Progr. Mater. Sci.* **21** (1976) 61.
2. K. A. PADMANABHAN and G. J. DAVIES, "Superplasticity" (Springer Verlag, Berlin, Heidelberg and New York, 1980).
3. F. JOVANE, *Int. J. Mech. Sci.* **10** (1968) 403.

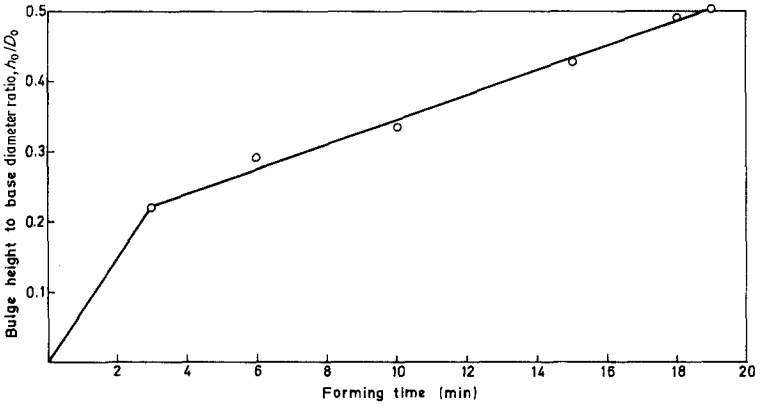

Figure 11 Bulge height as a function of forming time. Sn–Pb alloy. Initial sheet thickness = 1.3 mm. Forming pressure = 0.2 MPa. Hold-down load = 7.1 tonne.

4. T. Y. M. AL-NAIB and J. L. DUNCAN, *ibid.* **12** (1970) 463.
5. S. TANG and T. L. ROBBINS, *J. Eng. Mater. Technol. (Trans. ASME)* **96A** (1974) 77.
6. T. H. THOMSEN, D. L. HOLT and W. A. BACKOFEN, *Met. Eng. Quart.* **10** (2) (1970) 1.
7. W. A. BACKOFEN, I. R. TURNER and D. H. AVERY, *Trans. Amer. Soc. Met.* **57** (1964) 980.
8. R. HILL, *Phil. Mag.* **41** (1950) 1133.
9. H. W. SWIFT, *J. Mech. Phys. Solids* **1** (1952) 1.
10. P. B. MELLOR, *ibid.* **5** (1956) 41.
11. A. N. BRAMLEY and P. B. MELLOR, *Int. J. Mech. Sci.* 8 (1966) 101.
12. D. L. HOLT, *ibid.* **12** (1970) 491.
13. G. C. CORNFIELD and R. H. JOHNSON, *ibid.* **12** (1970) 479.
14. W. JOHNSON, T. Y. M. AL-NAIB and J. L. DUNCAN, *J. Inst. Met.* **100** (1972) 45.
15. G. G. W. CLEMAS, S. T. S. AL-HASSANI and W. JOHNSON, *Int. J. Mech. Sci.* **17** (1975) 711.
16. G. J. COCKS, G. ROWBOTTOM and D. M. R. TAPLIN, *Met. Technol.* **3** (1976) 332.
17. A. G. MAMALIS, W. JOHNSON and J. LEWIS, *ibid.* **4** (1977) 160.
18. D. LEE and W. A. BACKOFEN, *Trans. Met. Soc. AIME* **239** (1967) 1034.
19. F. JOVANE, A. H. SHABAIK and E. G. THOMSEN, *J. Eng. Ind. (Trans. ASME)* **91** (1969) 680.
20. T. OSHITA and H. TAKEI, *J. Jpn. Inst. Met.* **35** (1971) 1120.
21. J. L. DUNCAN and W. JOHNSON, *Int. J. Mech. Sci.* **10** (1968) 157.

Received 23 May
and accepted 4 June 1984